Optimal Stretching in Advection-Reaction-Diffusion Systems

Thomas D. Nevins[1,*] and Douglas H. Kelley[2,†]
[1]Department of Physics and Astronomy, University of Rochester, Rochester, New York 14627, USA
[2]Department of Mechanical Engineering, University of Rochester, Rochester, New York 14627, USA
(Received 27 April 2016; published 14 October 2016)

We investigate growth of the excitable Belousov-Zhabotinsky reaction in chaotic, time-varying flows. In slow flows, reacted regions tend to lie near vortex edges, whereas fast flows restrict reacted regions to vortex cores. We show that reacted regions travel toward vortex centers faster as flow speed increases, but nonreactive scalars do not. For either slow or fast flows, reaction is promoted by the same optimal range of the local advective stretching, but stronger stretching causes reaction blowout and can hinder reaction from spreading. We hypothesize that optimal stretching and blowout occur in many advection-diffusion-reaction systems, perhaps creating ecological niches for phytoplankton in the ocean.

DOI: 10.1103/PhysRevLett.117.164502

Introduction.—In advection-reaction-diffusion (ARD) systems, some quantity grows locally, spreads by random motions, and is carried along by the surrounding fluid flow. Many natural phenomena and industrial technologies are accurately described as ARD systems, including bulk chemical reactors [1], wildfires [2], combustion engines [3,4], microfluidic reactors [5], cellular growth [6], reaction in porous media [7,8], and phytoplankton ecology [9–11]. For any of these applications, improved understanding of ARD dynamics would allow forecasts of local and global concentrations and reaction rates. Practical impacts would include cleaner and more efficient combustion engines, more economical chemical manufacture, and more accurate prediction of phytoplankton populations.

We are particularly interested in studying ARD systems in which the reaction is both excitable, in that it proceeds only if the concentration exceeds some threshold, and autocatalytic, in that it spreads in fronts once triggered, because the reaction product is also a catalyst. Such reaction dynamics describe the oscillating Belousov-Zhabotinsky (BZ) chemical reaction [12–19], flame dynamics [12], and phytoplankton blooms [20,21].

In this Letter we will use results of ARD experiments to show that in excitable autocatalytic reactions, reacted regions have spatiotemporal dynamics that depend on characteristic flow speed—or in dimensionless terms, the Reynolds number. We observe that reacted regions primarily occupy vortex edges in low Reynolds number flows, but occupy vortex centers for high Reynolds number flows. We show that reaction fronts move toward vortex centers more quickly as the Reynolds number increases, but passive scalar fronts do not. Furthermore, we find that advective stretching rates [22], related to the finite time Lyapunov exponent (FTLE) [23], correlate with reaction state. The probability of a region being reacted is highest for moderate stretching rates, whereas strong stretching prevents the reaction and weak stretching does little to enhance reaction. Optimal stretching is ubiquitous in our experiments and likely occurs in excitable ARD systems generally. For example, regions of fast ocean flow may lack plankton because of strong stretching preventing reaction, and segregation of species into geographically distinct niches [24] may be explained by optimal stretching values that differ between species.

Methods.—We drive 2-mm-thick flows of the ferroin-catalyzed BZ reaction [12,25] by passing current through it over an array of magnets, as in Kelley and Ouellette [26], though our magnets are arranged in a checkerboard, not in stripes. The experimental vessel has a flat bottom with lateral dimensions 230×330 mm, and we avoid edge effects by observing only the central 150×200 mm. The apparatus has magnets spaced $L = 25.4$ mm and produces flows with Reynolds numbers $0 \leq \mathrm{Re} \leq 350$, where $\mathrm{Re} = UL/\nu$ (U is the measured root-mean-square velocity and ν is the kinematic viscosity). We measured $\nu = 1.6 \times 10^{-6}$ m^2/s using a TA Instruments DHR-2 rheometer. The Reynolds number compares inertial forces to viscous forces, and in our apparatus, we observe a transition from steady flow to time dependence at $\mathrm{Re} \sim 100$. When triggered, the BZ reaction oxidizes ferroin, changing from orange to blue [12]. BZ also produces other products that are catalysts for further reaction, making BZ autocatalytic. Diffusion spreads those catalysts, causing reacted regions to grow outward. Because BZ has a large Damköhler number [13], sharp fronts separate reacted and unreacted regions. We trigger reaction by immersing a silver wire near the vessel's center for 20 s, then initiating advection 30 s later.

To track both reaction state and advection (flow), we use two hardware-synchronized cameras (Emergent HS-4000M). One has a dichroic filter to pass blue light matching the color of the light-emitting diode illumination and the reacted BZ, so reacted regions appear bright. The other camera has a dichroic filter that blocks blue but passes

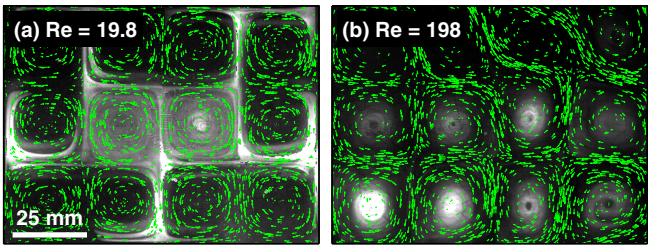

FIG. 1. Snapshots of ARD experiments with the BZ reaction. Arrows indicate the measured flow velocity. (a) In slow (Re = 19.8) flow, reacted regions persist near vortex edges, but (b) in fast (Re = 198) flow, reacted regions occupy vortex centers.

green, the color of the fluorescent tracer particles we add to the fluid to visualize advection. We measure advection by tracking each particle [27], typically 1000–8000 per experiment. Particles are 66 μm in diameter and follow fluid motions accurately. By simultaneously imaging a calibration pattern with both cameras, we determine their resolution (typically 170 μm/pixel) and the translational and rotational offsets between their images. Once the cameras are calibrated, we can overlay simultaneous measurements

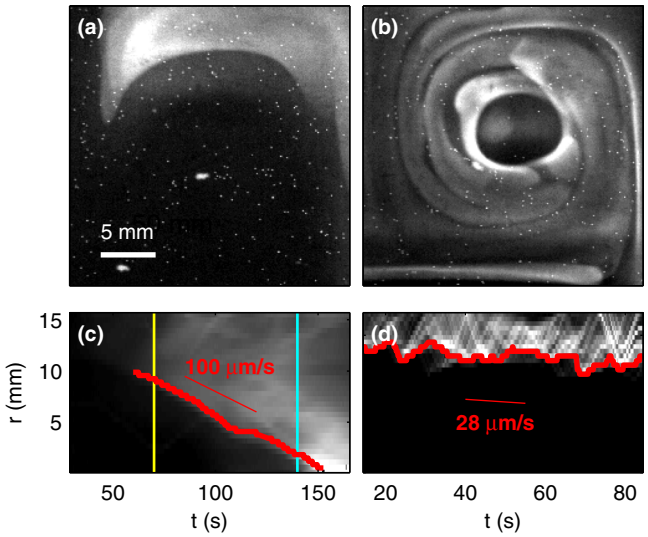

FIG. 2. Propagation of reacted regions toward vortex centers. (a) A reacted region entering a vortex at time $t = 70$ s. (b) The same vortex at $t = 140$ s, the bright reacted region has propagated inward. (c) Space-time plot showing azimuthally averaged brightness varying with radial position r and time t, in the vortex shown in (a) and (b). The thick curve marks the edge of the reacted region, and its slope measures the inward propagation speed, 103 μm/s. Vertical lines locate the snapshots in (a) and (b). Here, Re = 9.3. (d) Space-time plot generated by simulating a passive scalar in a vortex in a Re = 18.6 flow, with the edge and its slope indicated as in (c). The inward propagation speed of the passive region is nearly zero (in this experiment, 28 μm/s). Propagation toward vortex centers cannot be explained by advection alone.

of advection and reaction state. We adjust camera frame rates with flow speed.

Results.—First, we observe that reacted regions spend more time near vortex edges in low-Re flows, but prefer vortex centers in high-Re flows, as shown in Fig. 1. Supposing a smooth transition between these two distinct states, we would expect that reaction fronts move toward vortex centers with a speed that increases with Re. Figure 2 sketches our algorithm for measuring that speed. In each reaction state image we average the brightness of all pixels at a given radial distance from the center of the nearest vortex. The result is a measurement of azimuthally averaged brightness versus radius for each frame, and we display many subsequent frames on space-time plots. Using the Laplacian of a Gaussian edge finding method [28], we obtain the front location in each frame, and find that the reacted region always moves to smaller radii eventually. To show that the inward propagation of reacted regions is not trivially due to advection, we simulated the motion of a passive scalar in the same flow. In the simulation, we seeded the initially reacted region with tracers, then integrated the measured velocity fields to determine their trajectories. As shown in Fig. 2(d), we find little or no *radial* propagation of the passive scalar, consistent with an incompressible flow, but differing starkly from reacting material. (*Azimuthal* speed increases linearly with Re, as expected for passive tracers, or for reactions moving tangent to flow [29,30].) Thus, propagation of reacted regions toward vortex centers depends on coupling between reaction and advection (and possibly diffusion), and cannot be explained by advection alone.

With this algorithm we measure *inward radial* front speed at many different flow speeds, and for all reacted vortices not triggered by impurities, we obtain Fig. 3. We find that reacted regions do indeed propagate toward vortex centers more quickly as Re increases. The large variation in speed at each value of Re is not an indication of measurement error, nor time-varying advection, as all these experiments involve steady flow. Rather, it indicates variation in initial conditions: reacted regions first reach vortex edges at different times and places for each vortex.

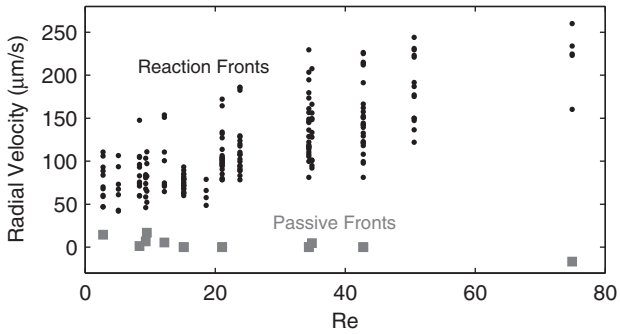

FIG. 3. Speed toward vortex centers increases with Reynolds number for reaction fronts, but not for a passive scalar.

Passive scalar fronts show negligible variation with Re, again demonstrating that the propagation of reacted regions toward vortex centers depends on coupling between reaction and advection. That observation is consistent with prior predictions that by spreading reacted regions, advection lengthens fronts and thereby drives diffusion, which supplies reactants more quickly and enhances reaction [31–33].

However, if advection always enhanced reaction, we would expect reacted regions to persist near vortex edges, where advection is fastest, even for large values of Re. Our observations show otherwise (Fig. 1). A transition occurs after which increased advection no longer enhances reaction, and it is natural to expect the transition to be governed by a quantifiable property of the flow. Such a property has been identified before in a simplified model. Neufeld [31] reduced a chaotic ARD system to a one-dimensional analytical model whose single flow parameter was the strain rate, which quantifies the rate at which regions of fluid are stretched by advection. He found that the spatially averaged reactant concentration at large time was maximized at moderate strain rates. Larger strain rates blew out the reaction, and smaller strain rates did little to enhance reaction. Though in that analytical model the strain rate was spatially uniform, the strain rate uniquely determines the stretching S, which can vary in space and time and can be measured in simulations and experiments. The stretching is a dimensionless, Lagrangian quantity defined as the largest eigenvalue of the right Cauchy-Green strain tensor [22], and is obtained from ϕ, the function that maps each point $\boldsymbol{x}_0$ in the flow at time t to its location $\boldsymbol{x}$ at time $t+T$. The Cauchy-Green strain tensor $C_T(\boldsymbol{x})$ is given by [34]

$$(C_T(\boldsymbol{x_0}))_{i,j} = [\nabla\phi_T]_{k,i}[\nabla\phi_T]_{k,j},$$

where

$$(\nabla\phi_T)_{i,j} = \frac{\partial x_i}{\partial x_{0,j}}.$$

The FTLEs commonly used for locating barriers to scalar mixing are defined as [22,23,35] $\lambda = T^{-1}\log S^{1/2}$. In the results described in this Letter, we consider S with $T = -15$ s, that is, the stretching imposed by the prior 15 s of advection. A consistent stretch time is essential so that in all experiments the physical meaning of the stretch, as experienced by the reaction, is maintained. The value $T = -15$ s corresponds to half an eddy turnover time in the slowest flows measured, and proved long enough for qualitative convergence of S, which depends only weakly on T if T is sufficiently large [36].

Recent numerical experiments have observed correlations between stretching and reaction rate. In simulations of the double-gyre flow, a two-dimensional prescribed model, the reaction rate was observed to be enhanced in regions of strong stretching [37]. When two competing autocatalytic species were simulated in double-gyre flow, it was observed that the one initiated in a region of stronger stretching almost always dominated long term [38]. Similarly, in simulations of competing species in sine flow, another two-dimensional prescribed model, it was observed that local FTLEs accurately predict long-term concentrations [1]. Experiments have shown that the global averaged FTLE is correlated with global reaction rate [39].

The chaotic advection we observe is not prescribed, but is produced physically using the described apparatus. Furthermore, we consider ongoing reaction state, not only long-term behavior. Nonetheless, the observed reaction state correlates with measured stretching, as shown in Fig. 4. The correlation changes with advection speed. For small values of Re, reacted regions lie primarily along vortex edges and in narrow filaments where stretching is strongest, consistent with simulations showing that stretching enhances reaction [1,37,38]. At large values of Re, however, reacted regions are confined where S is weakest. At moderate values of Re, reacted regions lie where stretching is moderate, away from both the large-S corners and the small-S vortex cores. In all cases, reacted regions lie where stretching has similar magnitude—an optimal range

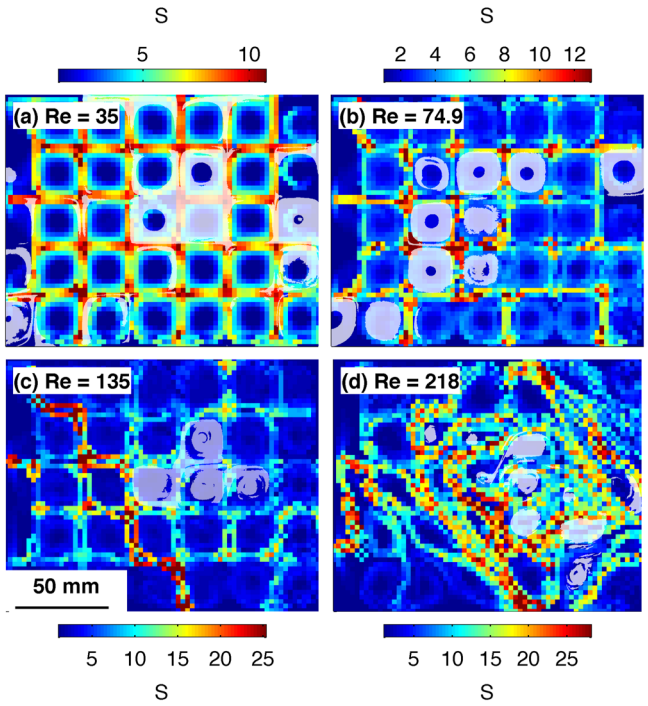

FIG. 4. Observed reaction state and measured stretching S overlaid for (a) Re = 35, (b) Re = 74.9, (c) Re = 135, and (d) Re = 218. Reacted regions are shaded lighter. The typical stretching in reacted regions is similar in all four experiments, but the range of stretching values increases with Re. Color scales vary. Stretching is calculated on a 2.5-mm grid, below our resolution but allowing sufficient data for stretching measurements at all grid points.

of S for enhancing reaction, consistent with Neufeld's simple model [31].

To quantify the relationship between stretching and reaction state, we calculate S throughout the observation region at all times after an initial 15 s, and compare the observed reaction state. As in Fig. 4, regions are classified as reacted or unreacted based on whether their brightness exceeds a chosen threshold. No reacted regions smaller than 5.8 mm^2 are considered. We make histograms of reacted and unreacted stretching values to estimate the probability $p(\text{reacted}|S)$ that a region with a given stretching will be reacted. The probabilities in three experiments are shown in Figs. 5(a)–5(c). These probabilities estimate a binomial distribution's probability parameter for each bin of S. Since S is usually small [22], estimation errors are highest for large S. Our analysis shows that for small values of Re, the probability of being reacted increases with stretching. For larger values of Re, larger values of S become available, but the probability there is low. This is the phenomenon we call blowout: regions with stretching stronger than some blowout level S_b allow little or no reaction. Such regions are visible in Figs. 4(b)–4(d). One striking example is shown in Fig. 4(c). In that experiment, reaction was triggered in the bright vortex just left of the center of the image, but did not spread farther left because of a blowout barrier, instead spreading right. We estimate $S_b \sim 15$ for BZ with $T = -15$ s, and we hope to measure S_b more precisely in future work.

Further support for the idea of optimal stretching comes from Fig. 5(d), where we plot the average stretching $\langle S \rangle$ for reacted and unreacted regions. For large values of Re, $\langle S \rangle$ is larger in unreacted regions, but for small values of Re, $\langle S \rangle$ is larger in reacted regions. Reacted regions persist at highest available S for low Re and at lowest available S for high Re. The transition between these two regimes occurs around Re ~ 70, and is not coincident with the transition to time-varying advection at Re ~ 100, so it is unlikely a consequence of advection alone.

Summary and implications.—We have observed that reacted regions primarily occupy vortex edges for small values of Re, but primarily occupy vortex cores for large values of Re. We found that as Re increases, reaction fronts move more quickly toward vortex cores. We explained our observations with stretching of material volumes, and showed that for the BZ, there exists an optimal range of S for enhancing reaction. Just as a flame grows in moderate winds but is blown out by high winds, moderate stretching promotes reaction by supplying fresh reactants, but strong stretching inhibits excitable reactions by diluting the catalyst.

Our results indicate that the key feature in the blowout of an excitable reaction is the presence of an excitation threshold, above which the reaction takes a long excursion away from equilibrium, but below which the system quickly returns to equilibrium. Material volumes in an incompressible fluid cannot change volume, only shape. Nor does reaction spread reactants. Therefore, diffusion is the only mechanism that can move reactants in and out of material volumes, and diffusion is enhanced when stretching increases the surface areas of material volumes. However, enhanced diffusion not only brings reactants more quickly, but also dilutes catalysts more quickly. With too much dilution, the excitable threshold is crossed in reverse, and blowout occurs.

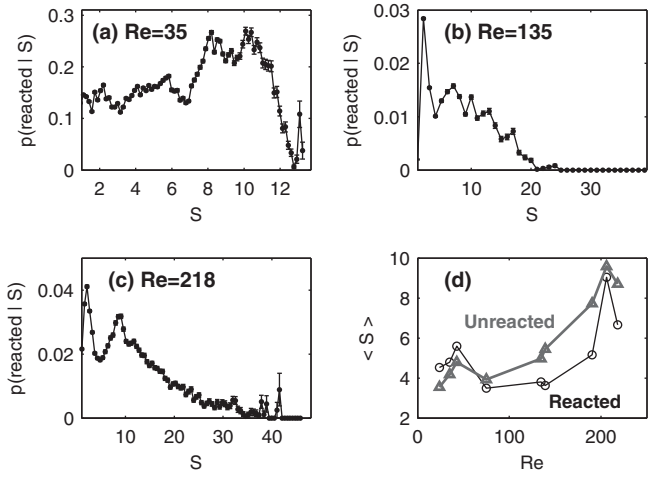

FIG. 5. Dependence of reaction state on stretching. (a)–(c) The probability $p(\text{reacted}|S)$ that a region with a given stretching S will be reacted, at varying Re. We calculate the probability by normalizing the number of reacted pixels with the given stretching by the total number of points with the given stretching. Because we plot no data point involving fewer than 100 measurements, the probabilities plotted as zero are well estimated by a probability of zero. We avoid transients by excluding the first 15 s of each experiment. (d) Average stretching $\langle S \rangle$ in reacted and unreacted regions over nine entire experiments, each at least 500 frames long, at varying Re; error bars are smaller than the plot markers. For Re < 70, reacted regions have larger $\langle S \rangle$, but for Re > 70, unreacted regions have larger $\langle S \rangle$. Flows with Re > 100 vary over time.

Though the regions of strong stretching, where $S > S_B$, account for only a small fraction of the total observation region, they can make large regions inaccessible to the reaction by blocking its spread. In large-Re flows, we observe that the reaction is often limited to a few vortices near the trigger point. In small-Re flows, however, the barriers are missing, and the initial reaction spreads throughout. Blowout could therefore represent a new sort of barrier to reactive mixing, in addition to the barriers predicted by theories of burning invariant manifolds (BIMs) and burning Lagrangian coherent structures (BLCS) recently developed by Mahoney and co-workers [14,15,40,41] and Megson *et al.* [16]. Both BIMs and BLCS are calculated using a constant reaction front speed and the flow ϕ. Those quantities alone are sufficient for locating barriers arising from interactions between front speed and advection speed—roughly, where front speed is

matched or exceeded by headwinds. Their power and simplicity are elegant. However, front speed is the only information about chemical kinetics encoded in BIMs and BLCS; the excitation threshold is absent. Thus, blowout would represent a new sort of barrier.

Blowout barriers likely occur in natural and industrial ARD systems outside the laboratory. For example, phytoplankton blooms may be blown out by fast ocean currents, and blowout regions may form barriers that segment the ocean. While plankton blooms depend on many conditions, they have been shown to be well modeled as excitable ARD systems [20,21] and are, therefore, likely to experience blowout. Blowout may play a role in forming the dynamical niches recently observed [24] to promote phytoplankton diversity in Earth's oceans.

In future work, we would first like to measure the optimal stretching range and blowout level more precisely and confirm that blowout causes reaction barriers. Second, we hope to perform experiments with simpler chemistry, to verify that blowout occurs only for excitable reactions, and not for other autocatalytic reactions. Third, the flows considered in this Letter are rotation dominated; it would be interesting to explore blowout in shear-dominated flow. Fourth, the correlation between stretching rate and reaction in low-Re flows seems to imply that the stretching field may relate quantitatively to the speed a reacted region grows. Therefore, it should be possible to use a stretching field to develop simplified time dynamics of mixed reaction. Finally, we would like to test our predictions for phytoplankton by applying these techniques to observational data from the ocean.

We are grateful to T. H. Solomon, J. Gore, R. F. Ashour, and K. Vats for insightful discussions.

*tnevins@ur.rochester.edu
†d.h.kelley@rochester.edu

[1] C. P. Schlick, P. B. Umbanhowar, J. M. Ottino, and R. M. Lueptow, Chaos **24**, 013109 (2014).
[2] C. Punckt, P. S. Bodega, P. Kaira, and H. H. Rotermund, J. Chem. Educ. **92**, 1330 (2015).
[3] S. Liu and C. Tong, Combust. Flame **162**, 4149 (2015).
[4] O. Kupervasser, Z. Olami, and I. Procaccia, Phys. Rev. E **59**, 2587 (1999).
[5] T. M. Squires and S. R. Quake, Rev. Mod. Phys. **77**, 977 (2005).
[6] G. L. Ryan, H. M. Petroccia, N. Watanabe, and N. Vavylonis, Biophys. J. **102**, 1493 (2012).
[7] S. Atis, S. Saha, H. Auradou, D. Salin, and L. Talon, Phys. Rev. Lett. **110**, 148301 (2013).
[8] S. Saha, S. Atis, D. Salin, and L. Talon, Europhys. Lett. **101**, 38003 (2013).
[9] A. P. Martin, Progr. Oceanogr. **57**, 125 (2003).
[10] M. Sandulescu, C. López, E. Hernández-García, and U. Feudel, Nonlinear Processes Geophys. **14**, 443 (2007).
[11] M. Sandulescu, C. López, E. Hernández-García, and U. Feudel, Ecol. Complex. **5**, 228 (2008).
[12] S. K. Scott, *Oscillations, Waves, and Chaos in Chemical Kinetics* (Oxford University Press, New York, 1994).
[13] S. Gowen and T. Solomon, Chaos **25**, 087403 (2015).
[14] J. Mahoney, D. Bargteil, M. Kingsbury, K. Mitchell, and T. Solomon, Europhys. Lett. **98**, 44005 (2012).
[15] J. R. Mahoney and K. A. Mitchell, Chaos **23**, 043106 (2013).
[16] P. W. Megson, M. L. Najarian, K. E. Lilienthal, and T. H. Solomon, Phys. Fluids **27**, 023601 (2015).
[17] A. von Kameke, F. Huhn, A. P. Muñuzuri, and V. Pérez-Muñuzuri, Phys. Rev. Lett. **110**, 088302 (2013).
[18] A. von Kameke, F. Huhn, G. Fernández-García, A. P. Muñuzuri, and V. Pérez-Muñuzuri, Phys. Rev. E **81**, 066211 (2010).
[19] V. Pérez-Muñuzuri and G. Fernández-García, Phys. Rev. E **75**, 046209 (2007).
[20] J. E. Truscott and J. Brindley, Bull. Math. Biol. **56**, 981 (1994).
[21] Z. Neufeld, Chaos **22**, 037102 (2012).
[22] G. A. Voth, G. Haller, and J. P. Gollub, Phys. Rev. Lett. **88**, 254501 (2002).
[23] G. Haller and G. Yuan, Physica (Amsterdam) **147D**, 352 (2000).
[24] F. d'Ovidio, S. D. Monte, S. Alvain, Y. Dandonneau, and M. Lévy, Proc. Natl. Acad. Sci. U.S.A. **107**, 18366 (2010).
[25] P. M. Wood and J. Ross, J. Chem. Phys. **82**, 1924 (1985).
[26] D. H. Kelley and N. T. Ouellette, Am. J. Phys. **79**, 267 (2011).
[27] N. T. Ouellette, H. Xu, and E. Bodenschatz, Exp. Fluids **40**, 301 (2006).
[28] J. R. Parker, *Algorithms for Image Processing and Computer Vision* (Wiley, Hoboken, NJ, 2010).
[29] B. F. Edwards, Phys. Rev. Lett. **89**, 104501 (2002).
[30] M. Leconte, J. Martin, N. Rakotomalala, and D. Salin, Phys. Rev. Lett. **90**, 128302 (2003).
[31] Z. Neufeld, Phys. Rev. Lett. **87**, 108301 (2001).
[32] Z. Neufeld, I. Z. Kiss, C. Zhou, and J. Kurths, Phys. Rev. Lett. **91**, 084101 (2003).
[33] Z. Neufeld and E. Hernández-García, *Chemical and Biological Processes in Fluid Flows: A Dynamical Systems Approach* (Imperial College Press, London, 2009).
[34] M. R. Allshouse and T. Peacock, Chaos **25**, 097617 (2015).
[35] G. Haller, Annu. Rev. Fluid Mech. **47**, 137 (2015).
[36] S. C. Shadden, F. Lekien, and J. E. Marsden, Physica (Amsterdam) **212D**, 271 (2005).
[37] W. Tang and C. Luna, Phys. Fluids **25**, 106602 (2013).
[38] W. Tang and A. Dhumuntarao, Phys. Fluids **27**, 076601 (2015).
[39] P. E. Arratia and J. P. Gollub, Phys. Rev. Lett. **96**, 024501 (2006).
[40] K. A. Mitchell and J. R. Mahoney, Chaos **22**, 037104 (2012).
[41] J. R. Mahoney and K. A. Mitchell, Chaos **25**, 087404 (2015).